A Stochastic Drift Counteraction Optimal Control Approach to Glider Flight Management

Ilya V. Kolmanovsky and Amor A. Menezes

***Abstract*— This paper formulates two stochastic optimal control problems to determine optimal glider flight management decisions that include a time-varying selection of glider ground speed and an amount of time to spend climbing in a randomly-encountered thermal. In the first problem, the objective is to maximize the expected glider range while maintaining glider altitude within given limits. In the second problem, the objective is to maximize the expected range in which the glider is able to follow a moving ground vehicle within a prescribed distance while maintaining glider altitude within given limits. Both problems are treated using stochastic drift counteraction optimal control. Simulation results are reported and discussed. The work has application to glider flight performance improvement, and to noiseless surveillance by unmanned air vehicles.**

I. Introduction

A. Motivation and Goals

THIS paper examines the glider flight management decisions that maximize gliding range and ground vehicle surveillance capability in the presence of uncertain thermal locations and strengths. Gliding range maximization is important in instances of engine failure of powered small aircraft, for competition glider flight, and for miniaturized unmanned air vehicles that utilize gliding to reduce power plant weight. Gliders are also a noiseless means of conducting ground vehicle surveillance for border patrol applications, and for nuclear and chemical plant security. The purpose of this paper is to apply a recently developed stochastic optimal control technique [1] to the two problems of gliding range maximization and ground vehicle surveillance.

B. Technical Approach and Related Literature

The technical approach employed in this work is that of stochastic drift counteraction optimal control [1], which maximizes a cost functional reflective of expected time-to-violate specified constraints or expected total yield before violation of specified constraints, while in the presence of significant disturbances that cause system states to drift. Such an optimal control law may be viewed as providing drift counteraction; hence, it is referred to as the stochastic drift counteraction optimal control.

Stochastic optimal control approaches to glider flight management have been previously described in [2] (using the theory of [3]) and [4]. The approaches and problems considered in the above references are different from the ones treated here. Soaring is itself a well-studied problem, with many results for *dynamic soaring* [5]–[10], where flight energy is provided by wind velocity gradients, orographic features and wind gusts, *static soaring* [11], [12], where flight energy is influenced by thermals (rising currents of air caused by uneven solar ground heating), updrafts and downdrafts (larger regions of lift and sink, respectively), and *trajectory generation and optimization* [13]–[20].

I. V. Kolmanovsky and A. A. Menezes are with the Department of Aerospace Engineering, the University of Michigan, Ann Arbor, MI 48109, USA ilya@umich.edu; amenezes@umich.edu

C. Paper Outline

The remainder of this paper is as follows. Section II specifies the two problems that are the focus of this work. Section III outlines the applicable theory. Section IV discusses the results obtained for a particular glider model parameterization. Lastly, Section V presents conclusions and suggests directions for future research.

II. Problem Formulation

A. Range Maximization Problem

We assume that the glider flight path is partitioned into segments, and we let Δs denote the distance of a single flight segment. In each flight segment, the glider can encounter a thermal with strength (altitude increase rate) w_2, and the glider can spend u_2 seconds climbing this thermal. We also assume that the glider flies each flight segment with longitudinal speed u_1 when outside the thermal. This results in the altitude change rate $(f(u_1)+w_1)$, where $f(u_1)$ is the the polar curve representing the sink rate of the glider in still air given the glider longitudinal speed u_1, and w_1 denotes the time rate of change of the altitude due to the updraft (or downdraft, if w_1 is negative).

The following update equations approximately model the glider's flight:

$$h^+ = h + (-f(u_1)+w_1)\frac{\Delta s}{u_1} + w_2 u_2, \tag{1}$$

$$t^+ = t + u_2 + \frac{\Delta s}{u_1}, \tag{2}$$

where h is the altitude at the start of a flight segment, t is the total time traveled prior to the start of the flight segment, h^+ is the altitude at the end of the flight segment, and s^+ is the total time traveled at the end of the flight segment. The variables u_1 and u_2 are control variables.

The variables w_1 (thermal strength) and w_2 (updraft strength) are determined by the flight and weather conditions, and are typically unknown *a priori*. In this paper, we employ a Markov Chain model to describe the evolution of thermal strength and updraft strength along the flight path. Specifically, we assume that a prediction of the probability distribution of thermal and updraft strength in the next flight

segment can be made once a thermal and updraft of certain strength in a given flight segment is encountered.

The objective of the stochastic range maximization problem is to determine a control law that maximizes the expected distance that the glider can travel within a given time, t_{max}, i.e., the expected distance that the glider can travel before the system states exit a prescribed set,

$$G = \{(h,t):\ h_{min} \le h \le h_{max},\ t \le t_{max}\}. \tag{3}$$

The constraint $h \ge h_{min}$ is imposed because the glider has to execute a landing maneuver upon descending to the minimum feasible altitude h_{min}. The altitude of the glider should also not exceed the maximum feasible altitude, h_{max}, that is typically determined by oxygen requirement laws or airspace ceiling restrictions.

B. Ground Vehicle Surveillance Problem

In this problem, the glider must fly so that a moving ground vehicle target is kept under observation. The formulation of this problem is similar to the formulation of the range maximization problem for the glider. The update equations are

$$h^+ = h + (-f(u_1) + w_1)\frac{\Delta s}{u_1} + w_2 u_2, \tag{4}$$

$$d^+ = d + w_3(u_2 + \frac{\Delta s}{u_1}) - \Delta s, \tag{5}$$

where h is the altitude at the start of a flight segment, d is the relative distance to the ground vehicle at the start of the flight segment, h^+ is the altitude at the end of the flight segment, and d^+ is the relative distance to the ground vehicle at the end of the flight segment. The ground vehicle velocity, w_3, varies according to a Markov chain model.

The objective of the stochastic ground vehicle surveillance problem is to determine the control law that maximizes the expected range before the system states exit a prescribed set,

$$G = \{(h,d):\ h_{min} \le h \le h_{max},\ d_{min} \le d \le d_{max}\}, \tag{6}$$

where d_{min} and d_{max} are the minimum and maximum relative distances, respectively, at which surveillance can be reliably conducted.

C. Markov Chain Uncertainty Modeling

A Markov Chain model is used to represent the evolution of w_1, w_2 and w_3. The transition probabilities of the Markov chain are defined as

$$p_{ij} = \Pr[w^+ \in W_i \mid w \in W_j], \tag{7}$$

with W_i, $i = 1,\ldots,m$, defining a partitioning of the feasible range of the uncertainty. As an approximation, specific values of $w^i \in W_i$ may be associated with each W_i.

The Markov chain approach to stochastic uncertainty modeling permits a prediction of the distribution of updraft and thermal strength that may be encountered in the next flight segment given the estimates of the updraft and thermal strength in the current flight segment. This approach also facilitates the development of control laws utilizing stochastic dynamic programming.

III. Drift Counteraction Optimal Control Law Construction

We consider a class of control problems for discrete-time nonlinear systems with stochastic disturbances,

$$x(t+1) = f(x(t), v(t), w(t)), \tag{8}$$

where $x(t)$ is a vector state, $v(t)$ is a vector control, and $w(t)$ is a vector disturbance, the value of which is known at the time instant $t \in \mathbb{Z}^+$ while future values are unknown. The control input must satisfy control constraints $v(t) \in U$, where U is a specified set, as well as additional state constraints of the form $(w(t), x(t)) \in G$. Unlike conventional control systems that are designed to respond to set-points, here the set G is specified so that if $(w(t), x(t)) \in G$, then the system performance is acceptable.

If the drift caused by the disturbance is large, there may exist a time at which constraint violation is unavoidable regardless of the control law. In such a case, a *Stochastic Drift Counteraction Optimal Control* (SDCOC) law can be constructed [1] to maximize the expected time that the system operates without violating $v(t) \in U$.

The disturbance $w(t)$ is modeled by a Markov chain with a finite number of states, $w(t) \in W = \{w^j,\ j \in J\}$. The transition probability from $w(t) = w^i \in W$ to $w(t+1) = w^j \in W$ is denoted by $p_{ij} = P(w(t) = w^j | w(t) = w^i)$. In [1], a more general case of state-dependent transition probabilities is also considered.

Our objective is to determine a control function $u(x,w)$, such that with $v(t) = u(x(t), w(t))$, a cost functional of the form,

$$J^{x_0,w_0,u} = \mathrm{E}_{x_0,w_0}[\tau^{x_0,w_0,u}(G)], \tag{9}$$

is maximized. Here, $\tau^{x_0,w_0,u}(G) \in \mathbb{Z}^+$ represents the first-time instant when the trajectory of $x(t)$ and $w(t)$, which is denoted by $\{x^u, w^u\}$, resulting from the application of the control $v(t) = u(x(t), w(t))$ with values in the set U exits the prescribed compact set G. Note that $\{x^u, w^u\}$ is a random process, $\tau^{x_0,w_0,u}(G)$ is a random variable, and $\mathrm{E}_{x_0,w_0}[\cdot]$ denotes the expectation conditioned on initial values of x and w, i.e., on $x(0) = x_0$ and $w(0) = w_0$.

A. SDCOC Law Construction

Given a state vector, x^-, and disturbance vectors, $w^-, w^+ \in W$, we define

$$\begin{aligned} L^u V(x^-, w^-) &\triangleq \mathrm{E}_{x^-,w^-}\left[V\left(f\left(x^-, u\left(x^-, w^-\right), w^-\right), w^+\right)\right] \\ &\quad - V(x^-, w^-), \qquad (10) \\ &= \sum_{j \in J} V\left(f\left(x^-, u\left(x^-, w^-\right), w^-\right), w^j\right) \cdot p_{i,j} \\ &\quad - V(x^-, w^-). \qquad (11) \end{aligned}$$

The SDCOC law, $u_*(x,w)$, and its value function, $V(x,w)$, yield the following set of sufficient conditions [1]:

$$\begin{aligned} L^{u_*} V(x,w) + 1 &= 0, \text{ if } (x,w) \in G, \\ L^u V(x,w) + 1 &\le 0, \text{ if } (x,w) \in G,\ u \ne u_*, \\ V(x,w) &= 0, \text{ if } (x,w) \notin G. \end{aligned} \tag{12}$$

The conditions (12) can be treated numerically using either a value iteration approach or a linear programming approach. In this paper, a value iteration approach is used, wherein a sequence of functions that converge to the value function is defined using the following iterative process:

$$V_0 \equiv 0,$$
$$V_n(x,w^i) = \max_{v\in U}\left\{\sum_{j\in J} V_{n-1}\left(f\left(x,v,w^i\right),w^j\right)p_{ij}+1\right\}, \quad (13)$$
$$\text{if } (x,w^i)\in G,\ n>0.$$

In [1] it is shown that this sequence of functions $\{V_n\}$ is monotonically non-decreasing and converges pointwise to $V_*(x,w^i) = J^{x,w^i,u_*}$; this convergence is uniform if J^{x,w^i,u_*} is continuous.

The value iterations (13) produce a sequence of value function approximations, V_n, at specified grid-points $x\in\{x^k,\ k\in K\}$, and a stopping criterion is $|V_n(x,w^i)-V_{n-1}(x,w^i)|\le\varepsilon$ for all $x\in\{x^k,\ k\in K\}$ and $i\in J$, where $\varepsilon>0$ is sufficiently small. In each iteration, once the values of V_{n-1} at the grid-points have been determined, linear or cubic interpolation may be employed to approximate $V_{n-1}(f(x^k,v^m,w^i),w^j)$ on the right-hand side of (13), where $v\in\{v^m,\ m\in M\}$ is a specified grid for v. Formally, the approximate value iterations can be represented as follows,

$$V_0(x^k,w^i)\equiv 0,$$
$$V_n(x^k,w^i) = \max_{v^m,\ m\in M}\left\{\sum_{j\in J} F_{n-1}\left(f\left(x^k,v^m,w^i\right),w^j\right)p_{ij}+1\right\},$$

where $F_{n-1}(x,w^i) = \text{Interpolant}[V_{n-1}](x,w^i)$, if $(x,w^i)\in G$, and $F_{n-1}(x,w^i)=0$, if $(x,w^i)\notin G$.

Once an approximation of the value function, V_*, is available, an optimal control law may be determined from the following relation:

$$u_*(x,w^i)\in \text{argmax}_{v\in U}\left\{\sum_{j\in J} V_*\left(f\left(x,v,w^i\right),w^j\right)p_{ij}\right\}. \quad (14)$$

IV. Glider Control Law Computation

A. Glider Description and Model Parameters

The model is parameterized for Schweizer Aircraft's SGS 2-33A, a common flight trainer in North America that was manufactured during the late 1960s and throughout the 1970s [21]. In addition to the popularity of this two-seat glider, our choice is based on the relative inferiority of the glider's soaring performance (or glide ratio) when compared to modern sailplanes and competition gliders; hence, the optimal stochastic flight management decisions made with this trainer glider and the above theory may facilitate achieving comparable cross-country distances to those attained by skilled hobby glider pilots in high-performance gliders with artificial aid. A third reason for the choice of aircraft is author familiarity with glider flight instruction on this aircraft.

The glider polar curve, depicted in Fig. 1 [22], determines the sink rate, $v_z = f(u_1)$, in still (no-wind) air versus the ground speed. In this plot, V_S designates the sink rate, v_z, and the airspeed V is taken to be u_1 (i.e., we assume a no-wind condition). The diagram also illustrates a best glide ratio (i.e., a best lift/drag ratio or L/D ratio) of 22.25:1, corresponding to 22.25 m of forward travel for every 1 m of descent, at V speeds of approximately 20.1 m/sec or 45 mph solo and 23.2 m/sec or 52 mph dual. A minimum sink V_S speed of 0.792 m/sec or 2.6 ft/sec is achieved at a V speed of 17.0 m/sec or 38 mph solo, and V_S = 0.945 m/sec or 3.1 ft/sec at V = 18.8 m/sec or 42 mph dual. Current glider data are available in [23]. The polar curve for the glider was approximated by a quadratic function of the longitudinal speed,

$$v_z[\text{ft/sec}] = 8.2582 - 0.2870u_1[\text{mph}] + 0.0038u_1[\text{mph}]^2.$$

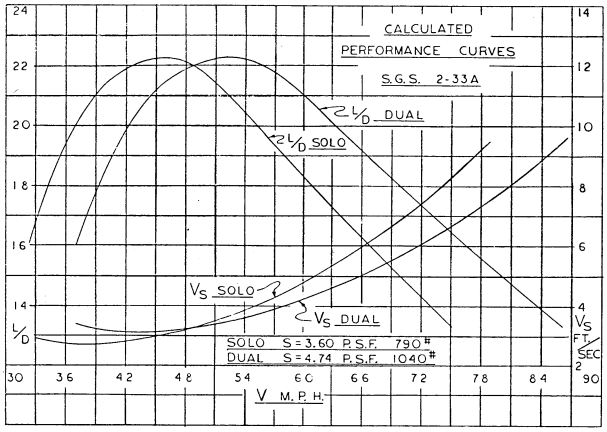

Fig. 1. Glide polar curve of the Schweizer SGS 2-33A [22].

The minimum and maximum altitudes for the glider were prescribed as $h_{min} = 1000$ ft and $h_{max} = 3000$ ft. For the value iterations, the altitude grid had a step size of 100 ft. In the maximum range problem, we assumed $t_{min} = 0$, $t_{max} = 1200$ s, and a grid step size of 30 s. In the ground vehicle surveillance problem, we assumed $d_{min} = -1800$ m, $d_{max} = 1800$ m and a grid step size of 150 m. In the range maximization problem, two thermal strength values of 0 and 1.67 ft/sec, and four updraft values of -6.6667, -3.3333, 0 and 1.6667 ft/sec were considered. The thermal strength and the updraft were treated as independent and their corresponding transition probability matrices,

$$P_1 = \begin{bmatrix} 0.8 & 0.2 \\ 0.8 & 0.2 \end{bmatrix},\ P_2 = \begin{bmatrix} 0.05 & 0.2 & 0.7 & 0.05 \\ 0.05 & 0.2 & 0.7 & 0.05 \\ 0.05 & 0.075 & 0.8 & 0.075 \\ 0.05 & 0.05 & 0.8 & 0.1 \end{bmatrix},$$

were combined. The thermal and updraft strength and probabilities were based on values of typical flight conditions encountered by the authors. Note that these transition probabilities imply that segments with no thermals and no updrafts/downdrafts are predominant. The grid points for the control variables (speed to fly outside the thermal and time to spend climbing the thermal) were chosen at 34, 39, 42, 45, 48, 54, 60, 66, 72, 78, 84 mph for u_1 and 0, 30, 60, 120, 180, 240, 300 sec for u_2.

In the ground vehicle surveillance problem, the ground vehicle velocity could take values of 39, 54 and 66 mph and the transition probability matrix has the following form

$$P_3 = \begin{bmatrix} 0.5 & 0.25 & 0.25 \\ 0.25 & 0.5 & 0.25 \\ 0.25 & 0.25 & 0.5 \end{bmatrix}.$$

The thermal strength model was the same as the range maximization case, with updrafts not considered for simplicity (the updraft speed was set to zero).

B. Range Maximization Results

The optimal value function (expected time to constraint violation) in the range maximization problem is in Fig. 2. Convergence of value iterations occurs after 35 iterations. Fig. 3 illustrates various cross-sections of the control policy.

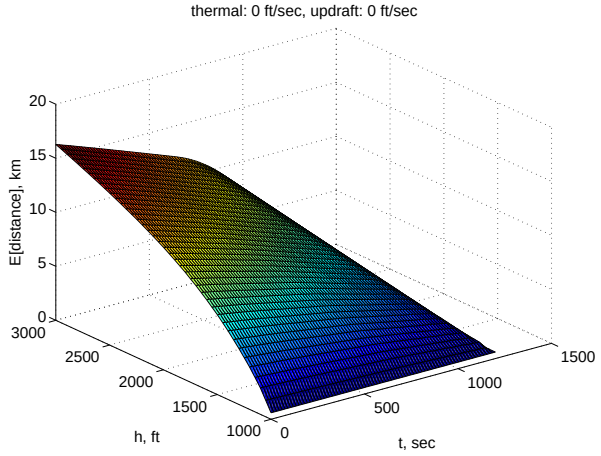

Fig. 2. Value function in the range maximization problem.

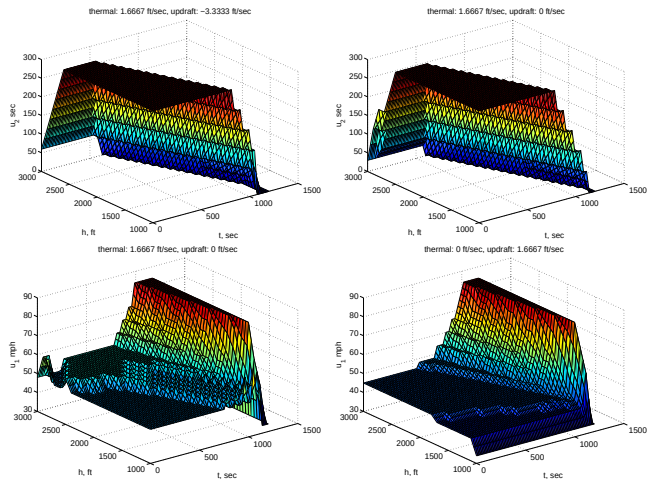

Fig. 3. Cross-sections of the control policy in the range maximization problem.

The following control policy trends are visible in Fig. 3 and the plots that follow. These trends are intuitive, and consistent with the general rules-of-thumb that are taught to glider student pilots for range maximization.

1) Thermals should be taken advantage of, even if located within a broader region of downdraft or sink (assuming sufficient pilot skill or automation and sufficient thermal diameter), as long as the glider is not close to violating the maximum height constraint and there is enough feasible flying time available.
2) Since greater sink rates can be accommodated at higher altitudes, speeds that are slightly faster than best L/D are permissible at these altitudes to increase the gliding range. If the flight time is close to the maximum flight time constraint, then an increased speed is desirable to gain more gliding range. The time at which to begin this speed increase depends on the available altitude.
3) A greater airspeed is desirable in regions of sink to quickly traverse these areas. A slower airspeed (i.e., the minimum sink speed) is desirable in regions of updraft to gain altitude.

Two simulation scenarios illustrate the above trends. In the first simulation scenario, the thermals are encountered relatively early during the glide, and in the second scenario, thermals are encountered only later during the glide.

Figs. 4–6 illustrate the time histories of the associated variables for the first simulation scenario. The red dashed lines indicate constraints, and the blue dots indicate snapshots of the flight conditions during a flight segment. The glider utilizes the first two thermals it encounters but skips thermals encountered later in the glide to avoid losing time in the thermals. Figs. 7–9 illustrate the time histories of the associated variables for the second simulation scenario. The glider travels faster through downdrafts, slower through updrafts, and close to the best L/D longitudinal speed value in flight segments without updrafts or downdrafts.

To provide additional context for the stated maximum distance gliding range values in Fig. 4 and Fig. 7, the glider descends from 2500 ft to 1000 ft in approximately 500 seconds at the best L/D speed of 46 mph without thermals or updrafts, thus covering a range of 10058.4 m in that time.

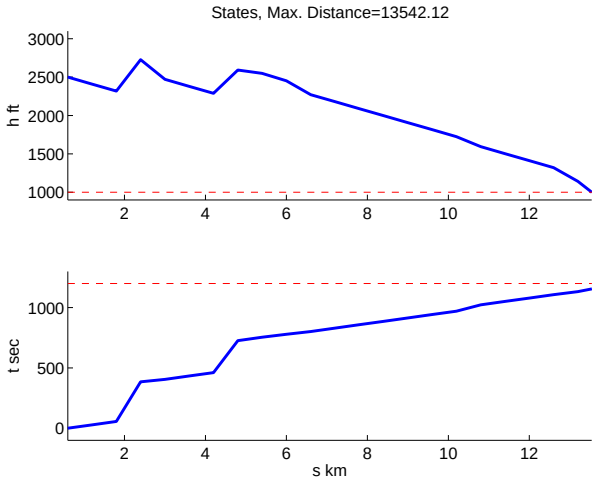

Fig. 4. Altitude and flight time of the glider versus distance in the range maximization problem, simulation scenario 1.

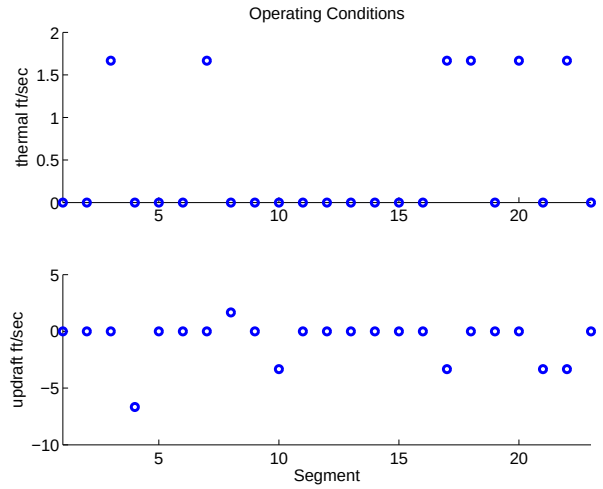

Fig. 5. Thermal strength and updraft versus flight segment number in the range maximization problem, simulation scenario 1.

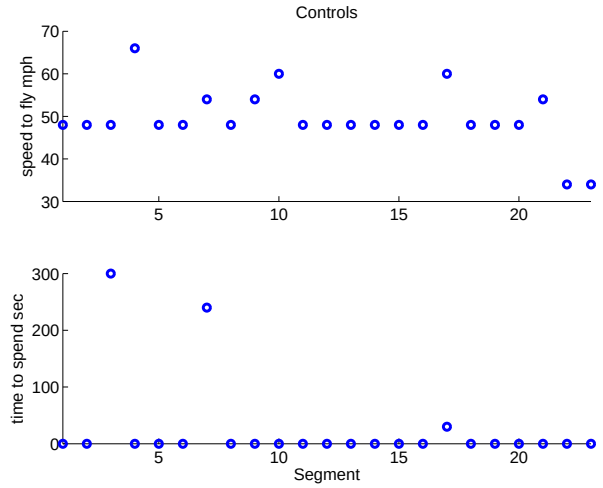

Fig. 6. Time to spend in a thermal and speed to fly versus flight segment number in the range maximization problem, simulation scenario 1.

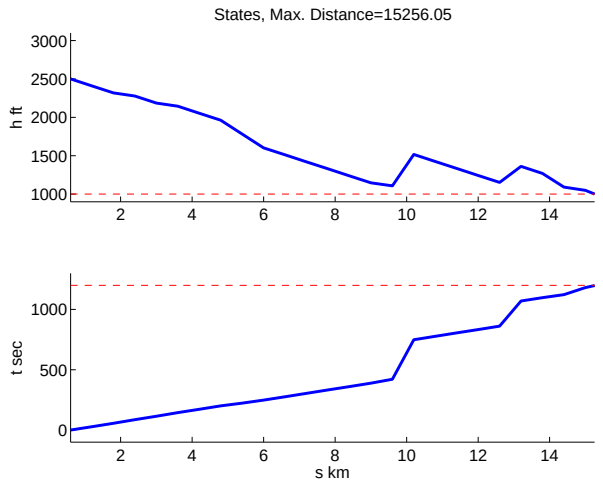

Fig. 7. Altitude and flight time of the glider versus distance in the range maximization problem, simulation scenario 2.

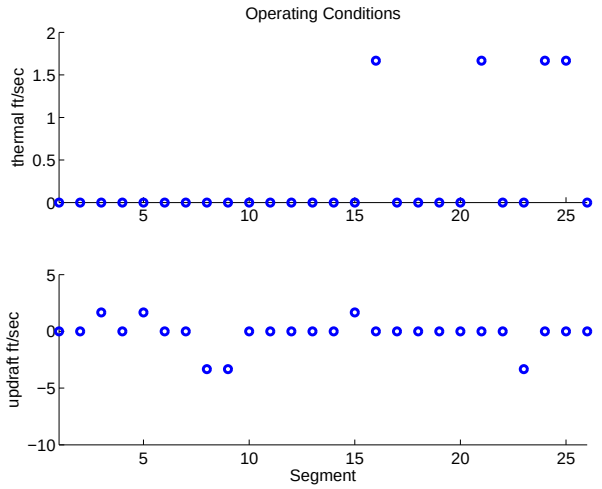

Fig. 8. Thermal strength and updraft versus flight segment number in the range maximization problem, simulation scenario 2.

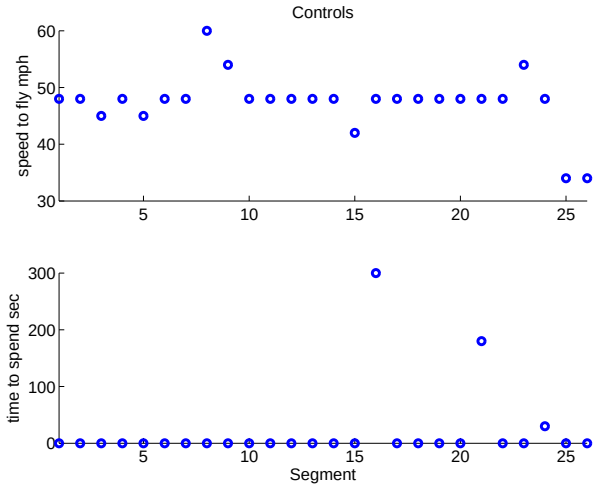

Fig. 9. Time to spend in a thermal and speed to fly versus flight segment number in the range maximization problem, simulation scenario 2.

C. Ground Vehicle Surveillance Results

In the simulation, the thermals are encountered relatively early during the glide (similar to Fig. 5). The time histories of the relevant variables are shown in Figs. 10–12. The red dashed lines indicate constraints, and the blue dots indicate snapshots of the flight conditions during a flight segment. The distance traveled is 11.42 km and, as expected, is less than the distance covered by the glider in the range maximization problem (13.54 km, see Fig. 4). The ground vehicle is initially behind the glider and moves at high speed with random speed changes. The glider takes advantage of two thermals along the flight path to reduce altitude loss. The ground vehicle moves ahead of the glider when the glider is delayed in the thermal. The glider chooses not to use three thermals encountered along the flight path.

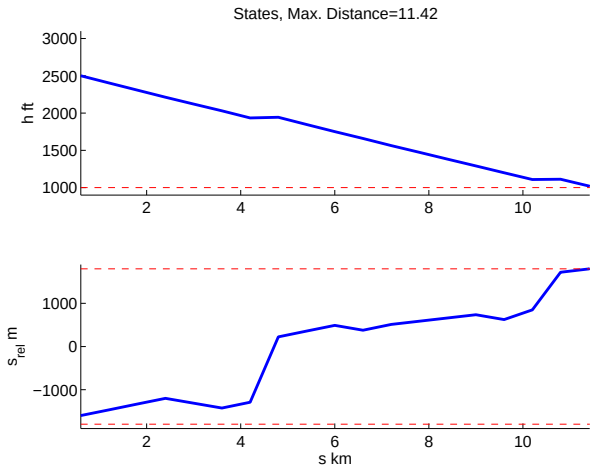

Fig. 10. Altitude and relative distance ($s_{rel} = d$) versus distance in the ground vehicle surveillance problem.

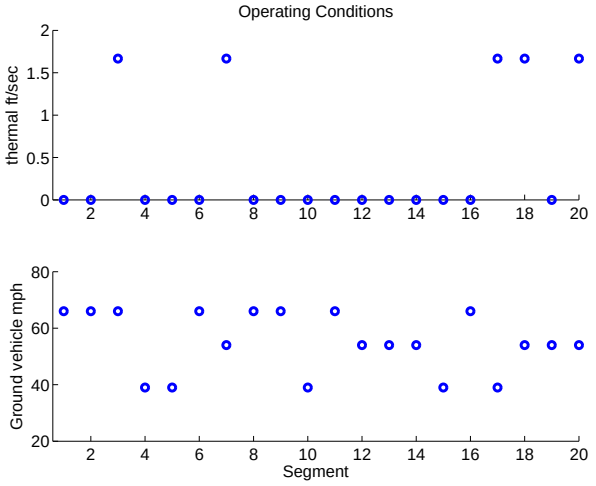

Fig. 11. Thermal strength and ground vehicle speed versus segment number in the ground vehicle surveillance problem.

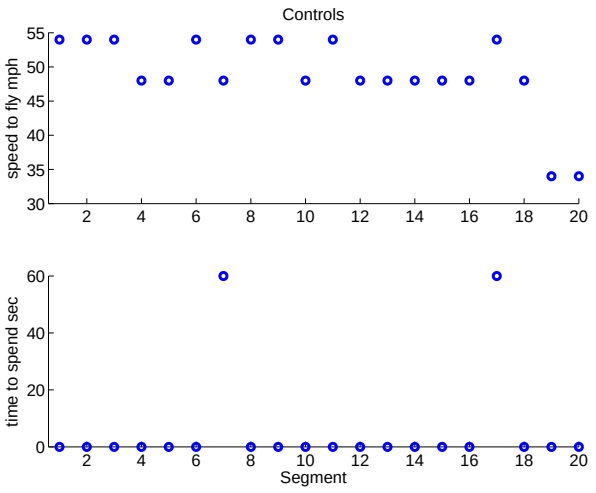

Fig. 12. Time to spend in a thermal and speed to fly versus flight segment number in the ground vehicle surveillance problem.

V. Conclusions

This paper has described and analyzed a gliding range maximization problem and a ground vehicle surveillance problem utilizing the recently developed technique of stochastic drift counteraction optimal control and a popular trainer glider in North America, the SGS 2-33A. The optimization results obtained with this technique from sample runs are intuitive and plausible.

References

[1] I. V. Kolmanovsky, L. Lezhnev, and T. L. Maizenberg, "Discrete-time drift counteraction stochastic optimal control: Theory and application-motivated examples," *Automatica*, vol. 44, pp. 177–184, January 2008.

[2] J. H. Cochrane, "MacCready theory with uncertain lift and limited altitude," *Technical Soaring*, vol. 23, pp. 88–96, July 1999.

[3] P. B. MacCready, Jr., "Optimum airspeed selector," *Soaring*, p. 10, January-February 1958.

[4] R. Almgren and A. Tourin, "Optimal soaring with Hamilton-Jacobi-Bellman equations," August 2004. [Online]. Available: www.courant.nyu.edu/ almgren/papers/optsoar.pdf

[5] F. Hendricks, "Dynamic soaring," Ph.D. dissertation, University of California, Los Angeles, 1972.

[6] G. Sachs and M. Mayrhofer, "Shear wind strength required for dynamic soaring at ridges," *Technical Soaring*, vol. 25, pp. 209–215, October 2001.

[7] T. Kiceniuk, "Dynamic soaring and sailplane energetics," *Technical Soaring*, vol. 25, pp. 221–227, October 2001.

[8] Y. J. Zhao, "Optimal patterns of glider dynamic soaring," *Optimal Control Applications and Methods*, vol. 25, pp. 67–89, March-April 2004.

[9] J. M. Wharington, "Heuristic control of dynamic soaring," in *Proceedings of the 5th Asian Control Conference*, vol. 2, 20–23 July 2004, pp. 714–722.

[10] C. K. Patel and I. Kroo, "Control law design for improving uav performance using wind turbulence," in *Proceedings of the 44th AIAA Aerospace Sciences Meeting and Exhibit*, 9–12 January 2006, pp. 1–10.

[11] M. J. Allen, "Autonomous soaring for improved endurance of a small uninhabited air vehicle," in *Proceedings of the 43rd AIAA Aerospace Sciences Meeting and Exhibit*, January 2005.

[12] M. J. Allen and V. Lin, "Guidance and control of an autonomous soaring vehicle with flight test results," in *Proceedings of the 45th AIAA Aerospace Sciences Meeting and Exhibit*, January 2007.

[13] R. Arho, "Optimal dolphin soaring as a variational problem," *OSTIV Publication XIII*, 1974.

[14] D. E. Metzger and J. K. Hedrick, "Optimal flight paths for soaring flight," *Journal of Aircraft*, vol. 12, pp. 867–871, 1975.

[15] H. Reichmann, *Cross-Country Soaring*. Thomson Publications, 1978.

[16] J. Sandauer, "Some problems of the dolphin-mode flight technique," *OSTIV Publication XV*, 1978.

[17] B. L. Pierson and J. L. D. Jong, "Cross-country sailplane flight as a dynamic optimization problem," *International Journal for Numerical Methods in Engineering*, vol. 12, pp. 1743–1759, 1978.

[18] G. Sander and F. X. Litt, "On global optimal sailplane flight strategy," in *Science and Technology of Low Speed and Motorless Flight*, P. W. Hanson, Ed. NASA, March 1979, no. NASA Conference Publication 2085, pp. 355–376.

[19] J. L. de Jong, "The convex combination approach: A geometric approach to the optimization of sailplane trajectories," *OSTIV Publication XVI*, pp. 182–201, 1981.

[20] J. W. Langelaan, "Long distance/duration trajectory optimization for small UAVs," in *Proceedings of the 2007 AIAA Guidance, Navigation and Control Conference and Exhibit*, no. AIAA 2007-6737, 16–19 August 2007.

[21] P. A. Schweizer, *Wings Like Eagles: The Story of Soaring in the United States*. Smithsonian Institution Press, 1988.

[22] *The 2-33 Sailplane Flight - Erection - Maintenance Manual*. Schweizer Aircraft Corporation.

[23] Department of National Defense, Canada, *Air Cadet Gliding Program Manual*, 2010, no. A-CR-CCP-242/PT-005.